A.alraddadi, et. al. International Journal of Engineering Research and Applications
www.ijera.com
ISSN: 2248-9622, Vol. 12, Issue 6, (Series-I) June 2022, pp. 01-08

RESEARCH ARTICLE OPEN ACCESS

Investigations of new material tellurite glasses TeO_2−TiO_2−ZnO for photon shielding applications.

A.alraddadi[1], B.Alasmari[1], H. Al-Atwi[1], A.Alzhrani[1], M.Al-Atwi[1], M.Albogami[1], H.Alshrary[1], S.Al-Atwi[1], F.laariedh[1], S.Alghamdi[1], S. Alfadhli[1].

ABSTRACT
In this paper, the photon-shielding parameters for tellurite-based glasses has been studied using GEANT4 toolkit under photon energy range from 10^{-3} to 10 MeV. Then were compared with the theoretical WinXCOM software for different concentrations (100-*x*-*y*)TeO2-*x*TiO2-*y*ZnO, (x,y)=(15,10) (15,5), (10,15), (10,10), (5,30) and (5,10) mol%. The examined attenuation properties were then utilized to calculate the $\mathbf{Z_{eff}}$ effective atomic number and the HVL half value layer and MFP mean free path of the radiation shielding glasses. The present results found the utilization of the new tested glasses are good promising materials for photon shielding applications.
Keys Words: photon-shielding, tellurite-based glasses, Mass attenuation coefficient (μ/ρ), Zeff, HVL, MFP.

Date of Submission: 20-05-2022 Date of Acceptance: 03-06-2022

I. INTRODUCTION

Although scientists have only known about radiation for a century, they have developed a wide variety of uses for this natural source. Today, for the benefit of mankind, radiation is used in medicine, industry and agriculture, as well as to generate electricity. Hospitals use a variety of nuclear materials and procedures to diagnose and treat a wide human disease such as Radiology, X-Ray machines, cancer therapy and others.

There is always a risk of damage to cells or tissue if exposed to any amount of ionizing radiation. Staff and patients might be put in grave danger if they are exposed to excessive levels of radiation. Over time, skin cells may be permanently damaged as a result of radiation exposure, cancer and other health problems and even death. [1]

Radiation is becoming a useful instrumentation in our daily life [2-7]. Therefore, much scientific research has been carried out to create a novel radiation shielding materials for human protection against these dangerous effects. [8-9] A material that can be employed as a protective material under high levels of nuclear radiation exposure is still needed.

These materials must possess specific characteristics, like high density, good thermal and structural properties where heat is easily dissipated, good resistance, shielding durability, availability, reusable with homogeneity quality, and effective cost to be a useful material are all factors to consider. Choice of these materials mainly based on its ability to reduce the exposure level by absorption or attenuation of sufficient amounts of incoming radiation.

To protect employees from radiations like as X-rays, gamma-rays, and neutrons, the most frequent materials used are lead and concrete. While lead continues to be a widely used source of radiation protection material because of its inexpensive cost and strong attenuation ability. However, the hazardous nature to human health of lead (Pb) and its environmental toxicity are serious problems encouraged scientists to investigate non-toxic alternatives [10-12].

The same for Concrete is commonly used as a barrier against high-energy photons, owing to its unique properties, structural flexibility and its density sufficiently efficient [13]. However, the concrete is impermeable to visible transmitted light, and it has various flaws, such as variations in substance and the creation of fissures due to water content. [14]

In this regard, various alternative glass, steel, composites, resins, alloys, and polymers, among other materials, can be used to shield against radiation, but only when the thickness is good enough to keep the radiation below safe levels.

Because of their transparency to visible light and the ability to modify their optical and physical properties and preparation methods, glass materials are especially ideal choices for use as g-rays and neutron radiation shielding in medical

services and nuclear research institutions [15-21]. [22-23]

Various heavy metal oxide glasses have been studied for their shielding and optical properties. By increasing the density of the materials, the adding of heavy metal oxides improves the attenuation achievement of the glass sample [24-27].

The aim of the present study is to investigate the radiation shielding properties of the suggested glass through photon energies from 1 keV to 10 MeV by GEANT4 toolkit.

II. MATERIALS AND METHODS

In this purpose, we investigate a collection of tellurite glasses having a certain composition of (100- x -y)TeO_2-xTiO_2-yZnO, (x, y)=(15, 10) (15, 5), (10, 15), (10, 10), (5, 30) and (5, 10) mol%, The names and densities of the glasses compositions used in this study listed in Table1.

2.1 Monte Carlo simulation Geant4

GEANT4 is a Monte Carlo toolset for radiation propagation. This toolset has applications in a several domains, likes radiation shielding, medical applications, high-energy and Astor-particle physics, [28].

To cover all nuclear and electromagnetic interactions that might happen if the radiation collides with the material shielding, GEANT4 covers a diverse range of physical models for radiation shielding research.

The G4EmPhysicsList class to manage the physical processes involving electrons and photons has adopted the conventional electromagnetic package. This package includes interactions between photons with energies ranging from 1 to 100 TeV.

G4PhotoElectric-Effect, G4Compton-Scattering, G4Rayleigh-Scatterin, and G4Gamma-Conversion are some of the basic photonic interactions that have been incorporated. To ensure appropriate precision in simulations, the value of the range cut, which is the minimal limit for secondary particle generation, has been changed to 0,01cm for all desired particles. The energy of gamma photons were defined as 0.001–10 MeV. Depending on the gamma-ray energy, the glass thickness ranged from 0.1 to 1 cm. The mass number, atomic number, densities and weight fractions of the glasses samples were also computed.

One million photons were launched at a glass sample target from a mono-energetic source in this experiment. A sodium iodide (NaI) detector was used to record the photons.

2.2 Radiation shielding properties

2.2.1 Mass attenuation coefficient (μ/ρ)

The mass attenuation coefficient (μ/ρ) is the basic parameter used to measure the radiation absorption properties of any material. The expression of mass attenuation coefficient (μ/ρ) is a metric for the probability of incident photons interacting with substance per unit density. According to Lambert–Beer law [29], The amount of attenuation is determined by the gamma-ray energy and the glass sample's chemical structure. The formula is used to compute it:

$$\mu/\rho=\sum_i w_i(\mu/\rho)_i$$

Where (μ) is the linear attenuation coefficient, (ρ) is the density and w_i is a percentage of weight of i^{th} composed element in the shielding material sample.

2.2.2 Effective atomic number (Z_{eff}):

The effective atomic number (Zeff) is a metric that is used to measure the efficiency of a shielding material that contains a variety of components. A greater Zeff number shows that the material can filter incoming radiation better, thus a glass system with a greater Zeff value may attenuate input photons better than one with a lower Zeff value. The effective atomic number (Zeff) for any sample is widely used to explain the sample's attenuation behavior, and it is provided by the relation below. [30]:

$$Z_{eff} = \frac{\sum_i f_i A_i (\frac{\mu}{\rho})_i}{\sum_j f_j A_j (\frac{\mu}{\rho})_j}$$

Where A_i is the atomic weight and Z_j is atomic number and μ/ρ is the mass attenuation coefficient, f_i is the fractional abundance of the element.

2.2.3 Half- value layer

The half-value layer is a highly important measure for studying gamma-ray shielding properties. and to judge the radiation efficiency of a material .

The half-value layer is the thickness that reduces the intensity of radiation by half and may be calculated. by the relation below [31].

$$HVL = \frac{\ln(2)}{\mu}$$

Where HVL Half-value layer and μ the linear attenuation coefficient.

2.2.4 Mean free path (MFP)

The mean free path (MFP) is the mean distance travelled by a photon inside a shielding material

prior to encountering an interaction, and can be obtained according to the equation [32]:

$$MFP = \frac{1}{\mu}$$

Where μ the linear attenuation coefficient and MFP Mean free path

2.2.5 Neutron removal cross section (ΣR)

The $\sum_R$ calculates the ability of the shielding material to reduce the neutrons by measurement the mass removal cross section $(\sum_{R/\rho})$ of substances that are compose the samples. $\sum_R$ is given by the relation below [33]:

To calculate $(\sum_{R/\rho})$ the mass removal cross section of substances that compose the samples $\sum_R$ used to determine the shielding material's ability to attenuate neutrons.

$$\sum R = \sum_i \rho_i \left(\sum R/\rho_i \right)$$

Where ρ_i is the partial density (g/cm³) of the i^{th} substance.

III. RESULTS AND DISCUSSION

Tellurite glasses TeO_2–TiO_2–ZnO with a composition of (100-x-y)TeO_2-xTiO_2-y ZnO, (x,y)= (15;10) (15;5), (10;15), (10;10), (5;30) and (5;10) mol%, used in this study listed in Table1.

The mass attenuation coefficient μ/ρ of these samples were calculated using the Geant4 toolkit and the WinXCOM application for photon energy ranging from 1 keV to 10 MeV. In Figure.1, the μ/ρ values were presented against photon energy. The μ/ρ values obtained from Geant4 simulations were compared to those calculated by the WinXCOM algorithm, as shown in Figure.2. The values of μ/ρ were used to determine the Z_{eff} values, Figure.3. In Figure.4, the Half-value layer values of the investigated glasses were calculated and plotted. In figure 5 the mean free path values were computed and plotted.

Table1: list of investigated glasses samples, chemical and atomic composition and density.

		Glasses Samples					
		T85T5Z10	T65T5Z30	T80T10Z10	T75T10Z15	T80T15Z5	T85T15Z10
Compositions (mol%)	TeO_2	85	65	80	75	80	75
	TiO_2	5	5	10	10	15	15
	ZnO	10	30	10	15	5	10
Atomic composition (wt.%)	O	0.206	0.206	0.211	0.212	0.217	0.217
	Ti	0.016	0.018	0.033	0.034	0.050	0.051
	Zn	0.044	0.148	0.046	0.070	0.023	0.047
	Te	0.734	0.628	0.710	0.684	0.710	0.685
Density (g/cm³)		5.490	5.420	5.420	5.410	5.440	5.400

3.1 Mass attenuation coefficient (μ/ρ)

In Figure.1, the mass attenuation coefficient declines when the photon energy rises due to partial photon interactions with the shielding material in different energy ranges. As a result, the μ/ρ values decrease in low-energy zone (10^{-3}-0.39 MeV) because the photoelectric absorption mechanism dominates at these energies. Then, because Compton scattering dominates in the middle energy zone (0.6-3.9 MeV), the μ/ρ value significantly decline. Following that, because the pair production process, μ/ρ values gradually increase in the high energy zone (3.9-10 MeV). It can also be seen in Figure.1 that the photoelectric effect causes some abrupt discontinuities around the K-edges of Titanium, Zinc, and Tellurium substance. Furthermore, the relationship between the μ/ρ value and the chemical structure of the sample indicates that gamma-rays are attenuated more in the samples with a high Te weight component. The μ/ρ values of T85T5Z10, for example, are larger than those of the other glasses tested. The reason for this is that T85T5Z10 sample includes 85 mol% TeO_2 (see Table 1). The TeO_2 concentration in the glasses T80T10Z10 and T80T15Z5 is the same. However, T80T10Z10 includes 10mol% ZnO, and T75T15Z5 includes 5mol% ZnO. As a result, the μ/ρ values for T80T10Z10 are larger than those for T75T15Z5.

In Figure 2 provides a comparison of μ/ρ using WinXCOM and Geant.4 programs calculation for 123, 357, 665, 844, and 1333 keV photon energies. For all of investigated sample, we found the mass attenuation coefficient. Then correlation factor (R^2) was determined to ensure that the theoretical and simulation data were linear. The R^2 for all glasses was found to be almost one.

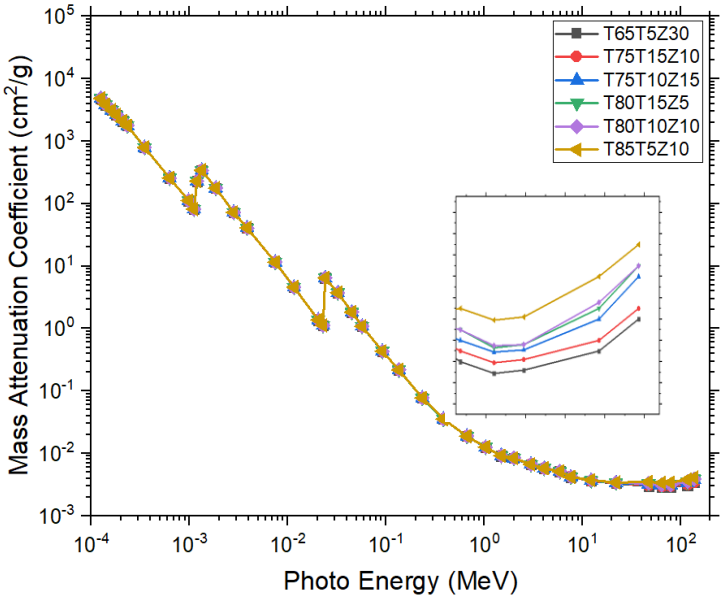

Fig. 1: TeO_2-TiO_2-ZnO glasses: Mass attenuation coefficient (μ/ρ) from 1 keV to 10 MeV

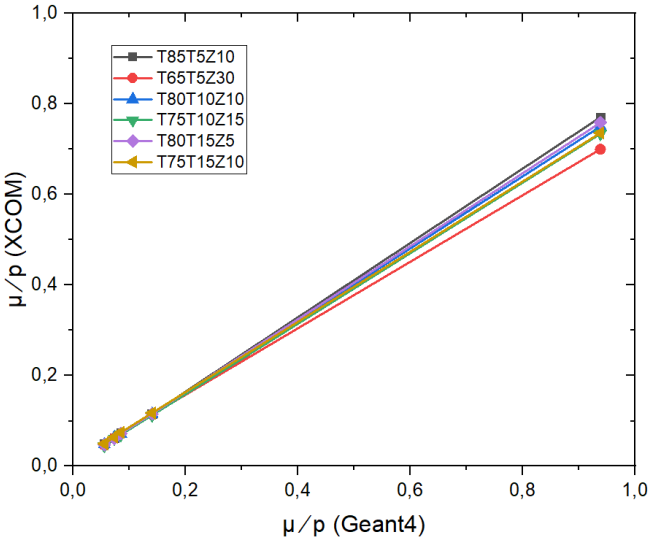

Fig. 2: Comparison of GEANT4 and WinXCOM mass attenuation coefficients for TeO_2-TiO_2-ZnO glasses.

3.2 Effective atomic number (Zeff)

Figure. 3 shows the computed Z_{eff} values for the examined tellurite-based glasses with various TeO_2 - TiO_2 and ZnO concentrations for photon energy zone from 10^{-3} to 1MeV.

When the photon energy is low, there is clearly an increase in Z_{eff} values. The (L, M, K) absorbed borders of titanium Ti, zinc Zn, and trillium Te components cause some peaks at 19–31 keV.

However, in the photon range of energies of 39–800 keV, the Z_{eff} values significantly drop as the photon energy increases. The values of the effective atomic number Z_{eff} for tellurite-based samples are then constant in the photon energy zone of 0.9-2 MeV because of the photoelectric interaction.

The Z_{eff} values gradually increase when the photon energy is increased up to 10MeV according to pair production process. Due to the atomic number (Z) of the material constituent atoms is significantly connected to the partial photon mechanisms; T85T5Z10 glass had the greatest Z_{eff} value, whereas T65T5Z30 glass had the lowest Z_{eff} value. As a result, the glass with the greatest Z_{eff} is T85T5Z10, which includes the largest weight

percentage of Te (0.734 percent). The T65T5Z30 glass, which has the smallest proportion of Te, has the lowest Z_{eff} (0.628 percent). It is commonly known that as Z_{eff} rises, so does the effectiveness of the gamma-ray shield.

As a result, we can conclude that the T85T5Z10 sample has the greatest gamma-ray shielding qualities of all the glasses we investigated. For comparison, we included the Z_{eff} for the current samples as well as those published for some other glass systems in Table 2.

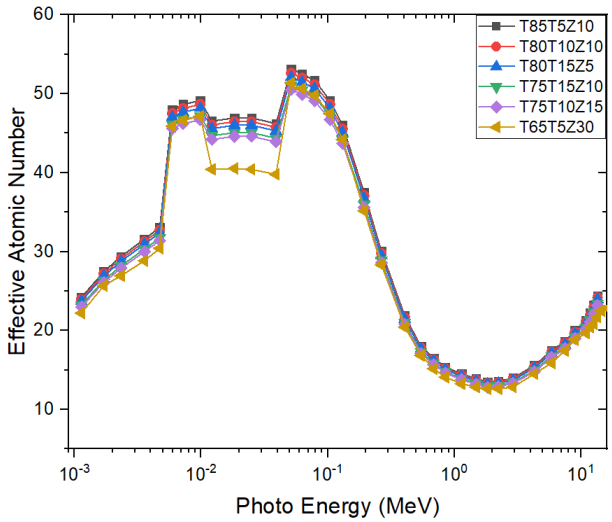

Fig. 3: Effective atomic number (Z_{eff}) of the TeO_2-TiO_2-ZnO samples for total photon interaction

Table 2 the effective atomic number Z_{eff} of investigated glasses samples.

Energy (MeV)	0.01	0.02	0.03	0.04	0.05	0.06	0.08	0.10	0.20	0.50	1.00	2.00	3.00	4.00	5.00	6.00	7.00	8.00	9.00	10.00
T85T5Z10	45.8	46.0	45.5	50.3	49.9	49.3	47.6	45.5	34.3	24.4	22.7	22.8	23.8	25.0	26.1	27.0	27.9	28.7	29.4	30.0
T65T5Z30	41.1	41.2	41.0	48.7	48.3	47.7	46.0	43.7	32.5	23.5	22.0	22.1	23.0	24.0	25.0	25.8	26.6	27.3	28.0	28.5
T80T10Z10	44.8	45.0	44.6	50.1	49.6	49.0	47.2	45.0	33.5	23.8	22.1	22.2	23.2	24.3	25.4	26.3	27.2	28.0	28.6	29.3
T75T10Z15	43.6	43.7	43.4	49.7	49.3	48.6	46.8	44.6	33.1	23.6	22.0	22.1	23.0	24.1	25.1	26.0	26.9	27.6	28.3	28.9
T80T15Z5	43.7	44.0	43.6	49.8	49.3	48.7	46.8	44.5	32.7	23.2	21.6	21.7	22.6	23.7	24.7	25.6	26.5	27.2	27.9	28.5
T85T15Z10	43.7	44.0	43.6	49.8	49.3	48.7	46.8	44.5	32.7	23.2	21.6	21.7	22.6	23.7	24.7	25.6	26.5	27.2	27.9	28.5

3.3 Half- value layer

The HVL is a key metric for determining gamma ray shielding performance (for better shielding efficiency must lower HVL). As shown in Figure. 4, the half value layer values of the samples investigated were compared to conventional glasses like barite concrete [34] and concrete [35].

The gamma-energy ray's determines how far it can penetrate through the shielding material. The glasses' half value layer ranged from 2 10^{-5} to 3.926 cm. Figure 4 clearly shows that for photon energies less than 0.1 MeV, the HVL values remain constant. Figure 4 demonstrates that the examined glasses have greater shielding qualities than either ordinary or barite concrete. Then, as the photon energy raises, the HVL values directly climb, peaking at 5 MeV.

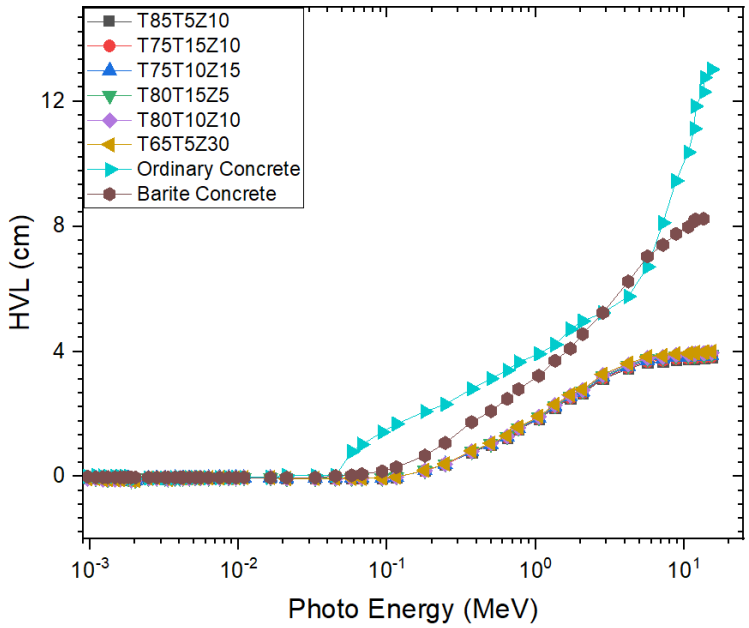

Fig. 4: Half-value layer (HVL) of the TeO_2-TiO_2-ZnO glasses compared with commercial concret.

3.4 Mean free path

The shields' capacity to block gamma-rays may be assessed by the MFP. The mean free path values of the glasses in investigation were determined and compared with a certain conventional shielding glasses Rs-253-G18, RS-520, and Rs-360 and present an exceptional gamma-ray shielding capability show in Figure 5. Obviously, at low photon energy, the MFP values of the current glasses are low. The values of MFP for all of the glasses increase greatly as the photon energy is increased. The thickness of these glasses must be raised in order for high-energy gamma rays to penetrate more deeply.

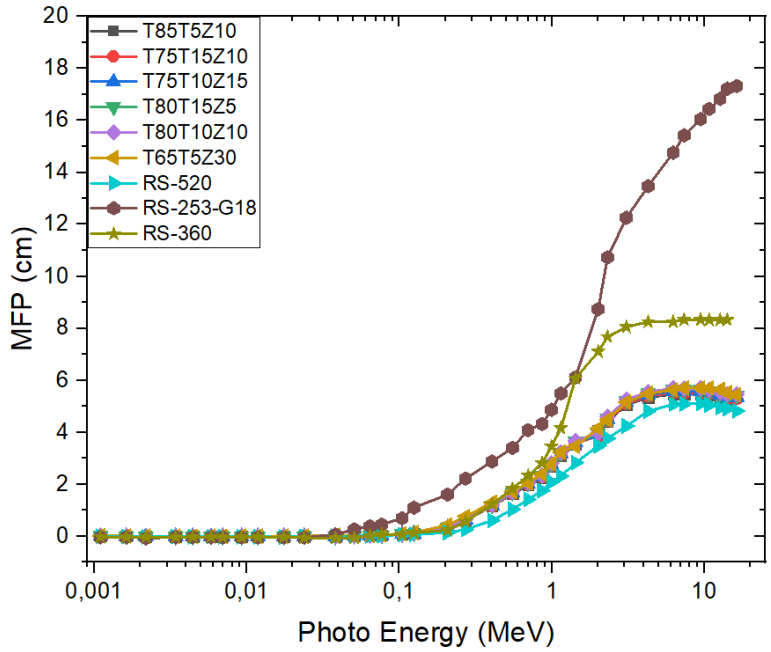

Fig. 5: Comparison of Mean free path of the TeO2-TiO_2-ZnO samples with commercial glasses

IV. CONCLUSION:

Tellurite-based glasses, TeO_2-TiO_2-ZnO have been studied for shielding protection against neutrons and gamma rays. The Geant4 toolkit and the WinXCOM software were utilized to determine the mass attenuation coefficient (μ/ρ) of these glasses confirmed with a correlation factor (R^2) equaling 0.999 after comparison. The greatest Z_{eff} values were found in the T85T5Z10 glass, while the lowest values were found in the T65T5Z30 glass, explained by the weight percentage of Te present in each sample. For photon energies range from 1 keV to 10 MeV, the half value layer of the investigated samples was calculated to be in the zone of 2.10^{-5} to 3.93 cm. In terms of Z_{eff}, HVL, and MFP, the shielding properties of investigated glasses were compared to commercial glasses and standard concrete and heavy metal oxide glasses. The suggested glass system was found to have good and potential alternatives for gamma and neutron shielding applications.

It is also possible to conclude that TeO_2 can be examined in the context of boosting nuclear radiation protection and other system properties.

ACKNOWLEDGMENT

The authors extend their appreciation to the deanship of Scientific Research at the University of Tabuk for funding this work through Research group no. S-1441–0151.

REFERENCES:

[1]. Akleyev, A.V. Normal tissue reactions to chronic radiation exposure in man. Radiat. Protect. Dosim. 71, 107–116. (2016)

[2]. Bagheri, Reza, Moghaddam, Alireza Khorrami, Shirmardi, Seyed Pezhman, Azadbakht, Bakhtiar, Salehi, Mojtaba. Determination of gamma-ray shielding properties for silicate glasses containing Bi2O3, PbO, and BaO. J. Non-Cryst. Solids 479, 62–71. (2018)

[3]. Sharifi, Sh, Bagheri, R., Shirmardi, S.P., 2013. Comparison of shielding properties for ordinary, barite, serpentine andsteel–magnetite concretes using MCNP-4C code and available experimental results. Ann. Nucl. Energy 53, 529–534.

[4]. Obaid, Shamsan S., Sayyed, M.I., Gaikwad, D.K., Pravina, P., 2018a. Pawar, attenuation coefficients and exposure buildup factor of some rocks for gamma ray shielding applications. Radiat. Phys. Chem. 148, 86–94.

[5]. Obaid, Shamsan S., Gaikwad, Dhammajyot K., Pawar, Pravina P., 2018b. Determination of gamma ray shielding parameters of rocks and concrete. Radiat. Phys. Chem. 144, 356–360.

[6]. Al-Hadeethi, Y., Sayyed, M.I., Rammah, Y.S., 2019. Investigations of the physical, structural, optical and gamma-rays shielding features of B2O3–Bi2O3–ZnO–CaO glasses. Ceram. Int. 45, 20724–20732.

[7]. Al-Hadeethi, Y., Sayyed, M.I., Rammah, Y.S., 2020a. Fabrication, optical, structural and gamma radiation shielding characterizations of GeO2-PbO-Al2O3–CaO glasses. Ceram. Int. 46, 2055–2062.

[8]. M.I. Sayyed, G. Lakshminarayana, I.V. Kityk, M.A. Mahdi, Evaluation of shielding parameters for heavy metal fluoride-based tellurite-rich glasses for gamma ray shielding applications, Radiat. Phys. Chem. 139 (2017) 33e39.

[9]. Ashok Kumar, Gamma ray shielding properties of PbO-Li2O-B2O3 glasses, Radiat. Phys. Chem. 136 (2017) 50e53.

[10]. Rashad, M., Ali, Atif Mossad, Sayyed, M.I., Somaily, H.H., Algarni, H., Rammah, Y.S., 2020. Radiation attenuation and optical features of lithium borate glasses containing barium: B2O3.Li2O.BaO. Ceram. Int. 46, 21000–21007.

[11]. Al-Hadeethi, Y., Sayyed, M.I., Mohammed, Hiba, Rimondin, Lia, 2020b. X-ray photons attenuation characteristics for two tellurite-based glass systems at dental diagnostic energies. Ceram. Int. 46, 251–257.

[12]. Dong, M.G., Sayyed, M.I., Lakshminarayana, G., Çelikbilek Ersundu, M., Ersundu, A.E., Nayar, P., Mahdi, M.A., 2017. Investigation of gamma radiation shielding properties of lithium zinc bismuth borate glasses using XCOM program and MCNP5 code. J. Non-Cryst. Solids 468, 12–16.

[13]. Zalegowski, Kamil, Piotrowski, Tomasz, Garbacz, Andrzej, Adamczewski, Grzegorz, 2020. Relation between microstructure, technical properties and neutron radiation shielding efficiency of concrete. Construct. Build. Mater. 235, 117389.

[14]. Lee, C.M., Lee, Y.H., Lee, K.J., 2007. Cracking effect on gamma-ray shielding performance in concrete structure. Prog. Nucl. Energy 49, 303–312.

[15]. C. Bootjomchai, J. Laopaiboon, C. Yenchai, R. Laopaiboon, Gamma-ray shielding and structural properties of bariumebismutheborosilicate glasses, Radiat. Phys. Chem. 81 (2012) 785e790.

[16]. S. Kaewjaeng, J. Kaewkhao, P. Limsuwan, U. Maghanemi, Effect of BaO on optical, physical and radiation shielding properties of

SiO2eB2O3eAl2O3eCaOe Na2O glasses system, Process Eng. 32 (2012) 1080e1086.
[17]. K.J. Singh, S. Kaur, R.S. Kaundal, Comparative study of gamma ray shielding and some properties of PbOeSiO2eAl2O3 and Bi2O3eSiO2eAl2O3 glass systems, Radiat. Phys. Chem. 96 (2014) 153e157.
[18]. A. Saeed, R.M. El shazly, Y.H. Elbashar, A.M. Abou El-azm, M.M. El-Okr, M.N.H. Comsan, A.M. Osman, A.M. Abdal-monem, A.R. El-Sersy, Gamma ray attenuation in a developed borate glassy system, Radiat. Phys. Chem. 102 (2014) 167e170.
[19]. M.I. Sayyed, Bismuth modified shielding properties of zinc boro-tellurite glasses, J. Alloy. Comp. 688 (2016) 111e117.
[20]. N. Chanthima, J. Kaewkhao, P. Limkitjaroenporn, S. Tuscharoen, S. Kothan, M. Tungjai, S. Kaewjaeng, S. Sarachai, P. Limsuwan, Development of BaOeZnOeB2O3 glasses as a radiation shielding material, Radiat. Phys. Chem. 137 (2017) 72e77.
[21]. Singh, K., Singh, H., Sharma, G., Gerward, L., Khanna, A., Kumar, R., Nathuram, R., Sahota, H.S., 2005. Gamma-ray shielding properties of CaO–SrO–B2O3 glasses. Radiat. Phys. Chem. 72, 225–228.
[22]. N.Chanthima, J.Kaewkhao, Investigation on radiation shielding parameters of bismuth borosilicate glass from 1 keV to 100 GeV, Annals of Nuclear Energy Vo- 55 (2013), P 23-28.
[23]. Sayyed, A.M.I., Elhouichet, H., 2017. Variation of energy absorption and exposure buildup factors with incident photon energy and penetration depth for boro-tellurite (B2O3-TeO2) glasses. Radiat. Phys. Chem. 130, 335–342.
[24]. F Laariedh, MI Sayyed, A Kumar, HO Tekin , Studies on the structural, optical and radiation shielding properties of (50–x) PbO–10 WO3–10 Na2O–10 MgO–(20+ x) B2O3 glasses, Journal of Non-Crystalline Solids 513 (2019), P159-166.
[25]. MI Sayyed, F Laariedh, A Kumr, MS Al-Buriahi, Experimental studies on the gamma photons-shielding competence of TeO2–PbO–BaO–Na2O–B2O3 glasses, Applied Physics A volume 126, 4 (2020).
[26]. M. I. Sayyed, M. H. A. Mhareb, Zinah Yaseen Abbas, Nouf Almousa, Farah Laariedh, Kawa M. Kaky, S. O. Baki Structural, optical, and shielding investigations of TeO 2–GeO 2–ZnO–Li 2 O–Bi 2 O 3 glass system for radiation protection applications, Applied Physics A volume 125, 417 (2019).
[27]. S. Agostinelli, J. Allison, K.a. Amako, J. Apostolakis, H. Araujo, P. Arce, M. Asai, D. Axen, S. Banerjee, G.. Barrand, et al., Nucl. Instr. Methods Phys. Res. Sect. A Accelerators Spectrometers Detect Assoc Equip 506(3), 250 (2003)
[28]. H. Tekin, E. Kavaz, E. Altunsoy, M. Kamislioglu, O. Kilicoglu, O. Agar, M. Sayyed, N. Tarhan, J. Non-Crystall. Solids 518, 92 (2019)
[29]. R. C. MURTY, Effective Atomic Numbers of Heterogeneous Materials Nature volume 207, pages398–399 (1965)
[30]. Louis K. Wagner,Benjamin R. Archer,Frank Cerra , On the measurement of half-value layer in film–screen\ mammography First published: November (1990)
[31]. David R. Penn, Electron mean-free-path calculations using a model dielectric function Phys. Rev. B 35, 482 – Published 15 January (1987)
[32]. R. E. Warner, F. Carstoiu, J. A. Brown, F. D. Becchetti, D. A. Roberts, B. Davids, A. Galonsky, R. M. Ronningen, M. Steiner, M. Horoi, J. J. Kolata, A. Nadasen, C. Samanta, J. Schwartzenberg, and K. Subotic, Reaction and proton-removal cross sections of on Si at 15 to 53 MeV/nucleon Phys. Rev. C 74, 014605 – Published 17 July (2006)
[33]. I. Bashter, Ann. Nucl. Energy 24(17), 1389 (1997)
[34]. I. Akkurt, H. Akyıldırım, B. Mavi, S. Kilincarslan, C. Basyigit, Ann. Nucl. Energy 37(7), 910 (2010)